

Review

Distributional Reinforcement Learning in the Brain

Adam S. Lowet,¹ Qiao Zheng,² Sara Matias,¹ Jan Drugowitsch,^{2,*} and Naoshige Uchida ^{1,*}

Learning about rewards and punishments is critical for survival. Classical studies have demonstrated an impressive correspondence between the firing of dopamine neurons in the mammalian midbrain and the reward prediction errors of reinforcement learning algorithms, which express the difference between actual reward and predicted mean reward. However, it may be advantageous to learn not only the mean but also the complete distribution of potential rewards. Recent advances in machine learning have revealed a biologically plausible set of algorithms for reconstructing this reward distribution from experience. Here, we review the mathematical foundations of these algorithms as well as initial evidence for their neurobiological implementation. We conclude by highlighting outstanding questions regarding the circuit computation and behavioral readout of these distributional codes.

Biological and Artificial Intelligence

The field of artificial intelligence (AI) has recently made rapid progress in algorithms and network architectures that solve complex tasks [1–4]. These advances in AI raise new questions in neurobiology, centered on the relationship between these state-of-the-art *in silico* learning algorithms and their biological counterparts in the brain [5]. Here, we discuss a new family of algorithms, termed **distributional reinforcement learning** (distributional RL; see [Glossary](#)) [6,7]. A recent study suggests that the brain's reward system indeed uses distributional RL [8], opening up opportunities for fruitful interactions between AI and neuroscience.

In this review, we first provide an overview of the basic algorithms of distributional RL and show how they can be understood from the single, unified perspective of regression. Next, we examine emerging neurobiological evidence supporting the idea that the brain uses distributional RL. Finally, we discuss open questions and future challenges of distributional RL in neurobiology.

Development of Distributional Reinforcement Learning in AI

The field of RL studies the algorithms by which an agent (e.g., an animal or computer) learns to maximize the cumulative reward it receives [9]. One common approach in RL is to predict a quantity called **value**, defined as the mean discounted sum of rewards starting from that moment and continuing to the end of the episode under consideration [9]. Predicting values can be challenging if the number of **states** is large and the value-function is nonlinear. A recent study overcame these challenges by combining past RL insights with modern artificial neural networks to develop an algorithm referred to as deep Q-network (DQN), which reached human-level performance in complex video games [2] ([Figure 1A,B](#)).

Various algorithms have been developed to improve upon DQN [10], including distributional RL [6,7]. The key innovation of distributional RL lies in how these algorithms predict future rewards. In environments where rewards and state transitions are inherently stochastic, traditional RL algorithms learn to predict a single quantity, the mean over all potential rewards. Distributional RL

Highlights

A large family of distributional RL algorithms emerges from a simple modification to traditional RL and dramatically improves performance of artificial agents on AI benchmark tasks. These algorithms operate using biologically plausible representations and learning rules.

Dopamine neurons show substantial diversity in reward prediction error coding. Distributional RL provides a normative framework for interpreting such heterogeneity.

Emerging evidence suggests that the combined activity of dopamine neurons in the VTA encodes not just the mean but rather the complete distribution of reward via an expeltilite code.

¹Department of Molecular and Cellular Biology, Center for Brain Science, Harvard University, Cambridge, MA 02138, USA

²Department of Neurobiology, Harvard Medical School, Boston, MA 02115, USA

*Correspondence: jan_drugowitsch@hms.harvard.edu (J. Drugowitsch) and uchida@mcb.harvard.edu (N. Uchida).



algorithms, by contrast, learn to predict the entire probability distribution over rewards (Figure 1C). Notably, modifying DQN to implement variants of distributional RL boosts performance by as much as two and a half times [6,7,10] (Figure 1D).

How Distributional RL Works

Two major topics in distributional RL are: (i) how the reward distribution is represented, and (ii) how it is learned. The original distributional RL algorithm [6] used data structures akin to histograms (the number of samples falling into fixed bins, or categories) to represent a distribution and treated learning as a multiclass classification problem. This class of distributional RL is hence called ‘categorical’ distributional RL [6]. Although using a histogram is an intuitive (and common) way to represent a distribution, it remains unclear whether neurons in the brain can instantiate this approach. A subsequent paper proposed to replace the histogram representation by an algorithm called **quantile regression** [7], which uses a novel population coding scheme to represent a distribution and a biologically plausible learning algorithm to update it.

Learning from Prediction Errors

One of the key ideas in RL is that learning is driven by prediction errors (i.e., the discrepancy between actual and expected outcomes) [11,12]. This idea originated in animal learning theories and was formulated mathematically by Rescorla and Wagner [13]. The Rescorla-Wagner (RW) rule postulates that the strength of association between two stimuli is updated based on a prediction error. In the simplest case, when a stimulus (X) is presented, the animal predicts the value of the future outcome. Once this outcome is revealed, the animal compares the outcome (R) against the predicted value (V) and computes the prediction error $\delta := R - V$. According to the RW rule, the value of stimulus X is updated in proportion to the prediction error:

$$V \leftarrow V + \alpha \cdot \delta. \quad [1]$$

Here, α is the learning rate parameter, which takes a value between 0 and 1. Equation 1 defines how the value V is updated. (The arrow indicates that V on the left-hand side is the value after updating whereas V on the right-hand side is the value before.) If R is constant, the predicted value gradually approaches the actual value and the prediction error approaches 0. Even if R is probabilistic, the predicted value will converge to the mean reward amount, at which point positive and negative prediction errors will balance across trials (Figure 2A). In a more sophisticated RL algorithm called **temporal difference (TD) learning** [9,11,12], the prediction error is computed based on the difference between the predicted values at consecutive time points (Box 1), but the update rule may otherwise remain the same.

Toward Distributional RL

While expected values can be useful, summarizing a situation by just a single quantity discards information that may become important in the future. If the demands of the animal change, for example, if large, uncertain rewards become preferred to smaller, certain ones [14], animals that store more detailed information about outcomes may perform better. Learning entire distributions sounds computationally expensive, but interestingly, distributional RL can arise out of two simple modifications to Equation 1 [7,8].

The first modification is to ‘binarize’ the update rule as follows,

$$V \leftarrow V + \alpha \cdot \begin{cases} -1 & \text{if } \delta \leq 0 \\ 1 & \text{if } \delta > 0 \end{cases} \quad [2]$$

Glossary

Distributional reinforcement learning:

a family of algorithms whereby an agent learns not only the expected reward, but rather the entire distribution of rewards.

Expectile: the τ -th expectile of a distribution is the value e_τ that minimizes the expectile regression loss function for τ (Equation 11). The 0.5-th expectile equals the mean.

Gradient: the gradient of a scalar-valued function f is a vector-valued function whose components are the partial derivatives of f . In this paper, f is a loss function with K model parameters to be optimized as its variables. Evaluating the gradient therefore results in a K -vector, which indicates how sensitive f is locally to small changes of the parameters.

Loss function: also called cost, error, or objective function, it is the equation that provides a metric for the goodness-of-fit of a set of parameters to data. One can fit a model, for example, a regression, by finding the parameters that minimize the loss function.

Markov dynamics: property of a state space such that the probability of a successor state s_{t+1} depends directly on s_t and not any prior state: $P(s_{t+1}|s_0, s_1, \dots, s_t) = P(s_{t+1}|s_t)$.

Nonparametric code: a type of population code that makes no assumptions about the underlying type of distribution. A quantile-like code is one example.

Parametric code: a type of population code in which neural activity reflects particular parameters of a predefined type of distribution (in simple cases, the mean and variance of a Gaussian, but often more complex distributions).

Population code: the representation of a particular type of information (e.g., the presence of a specific sensory stimulus, the average reward, or the distribution of rewards) by the firing of a population of neurons.

Quantile: the τ -th quantile of a distribution is the value q_τ such that τ fraction of samples is below q_τ , while the other $1 - \tau$ fraction is above it. Equivalently, q_τ minimizes the quantile regression loss function for τ (Equation 9). The 0.5-th quantile is the median.

Quantile regression: a model that predicts quantiles of a distribution given some predictor variables (e.g., a state vector).

Reinforcement learning (RL): a field of AI and theoretical neuroscience that

That is, the prediction error (δ) in the update equation is replaced by +1 or -1, depending on the sign of δ , such that value predictions are incremented (or decremented) by a fixed amount. In this case, V will converge to the median rather than the mean of the reward distribution (Figure 2B). Intuitively, this is because the median is the value that divides a distribution such that a sample from the full distribution is equally likely to fall above or below it. The increments and decrements specified by Equation 2 will balance out at the point where positive and negative prediction errors occur with exactly the same frequency, which is to say, when V is the median of the reward distribution.

The second modification is to add variability in the learning rate (α). Suppose we have a family of value predictors, V_i , each of which learns its value prediction in a slightly different way [7,8]. We assign each V_i two separate learning rates, an α_i^+ for positive prediction errors and an α_i^- for negative prediction errors, resulting in the learning rule

$$V_i \leftarrow V_i + \begin{cases} \alpha_i^- \cdot (-1) & \text{if } \delta_i \leq 0 \\ \alpha_i^+ \cdot (+1) & \text{if } \delta_i > 0 \end{cases} \quad [3]$$

considers the interaction between an agent and its environment. The agent receives states and rewards as inputs. It then takes actions that may modify its state and/or elicit reward. The agent's objective, in general, is to maximize value.

States: the description of the environment that is input to RL algorithms, alongside rewards.

Stochastic gradient descent: minimization method that computes the gradient of the loss function on individual samples, selected at random, and then adjusts the parameters in the negative direction of this gradient.

Temporal difference (TD) learning: bootstrapping technique in RL that computes the difference between predicted value at successive points in time to update the estimate of value.

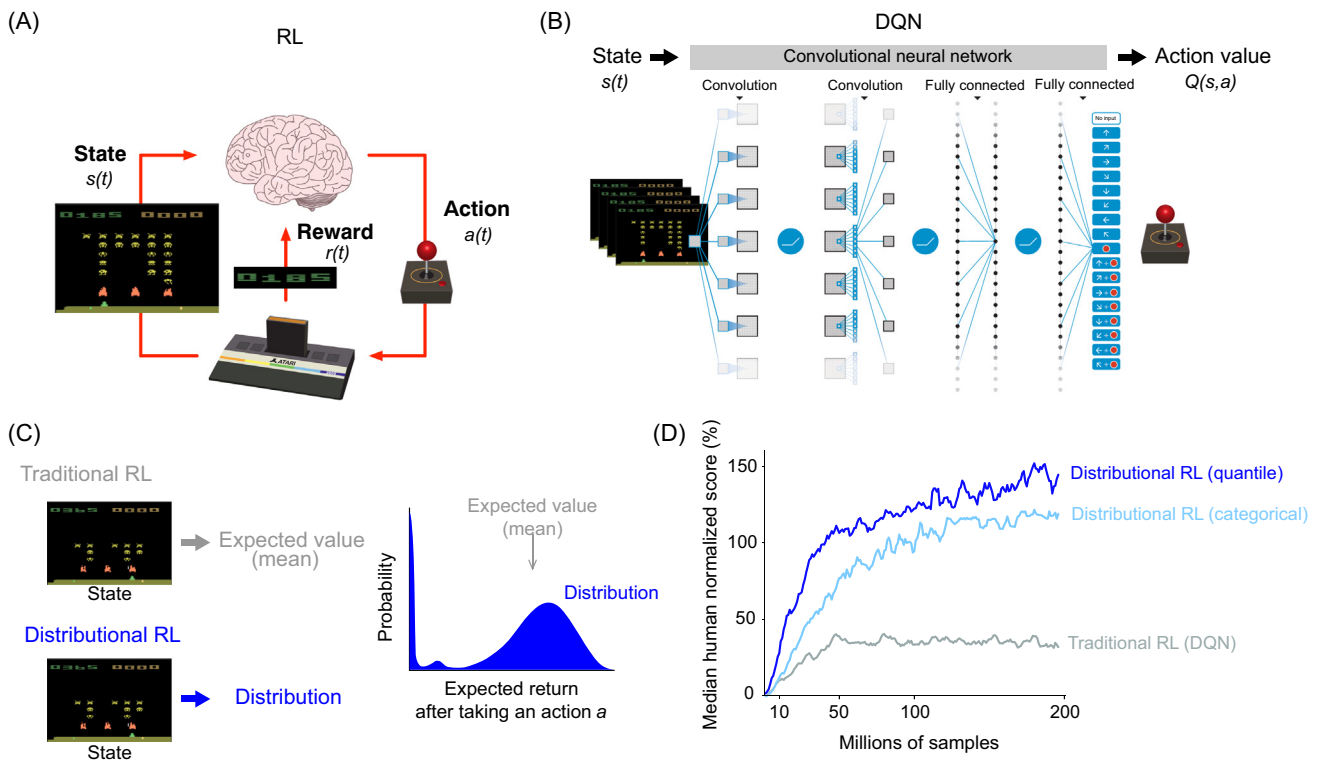
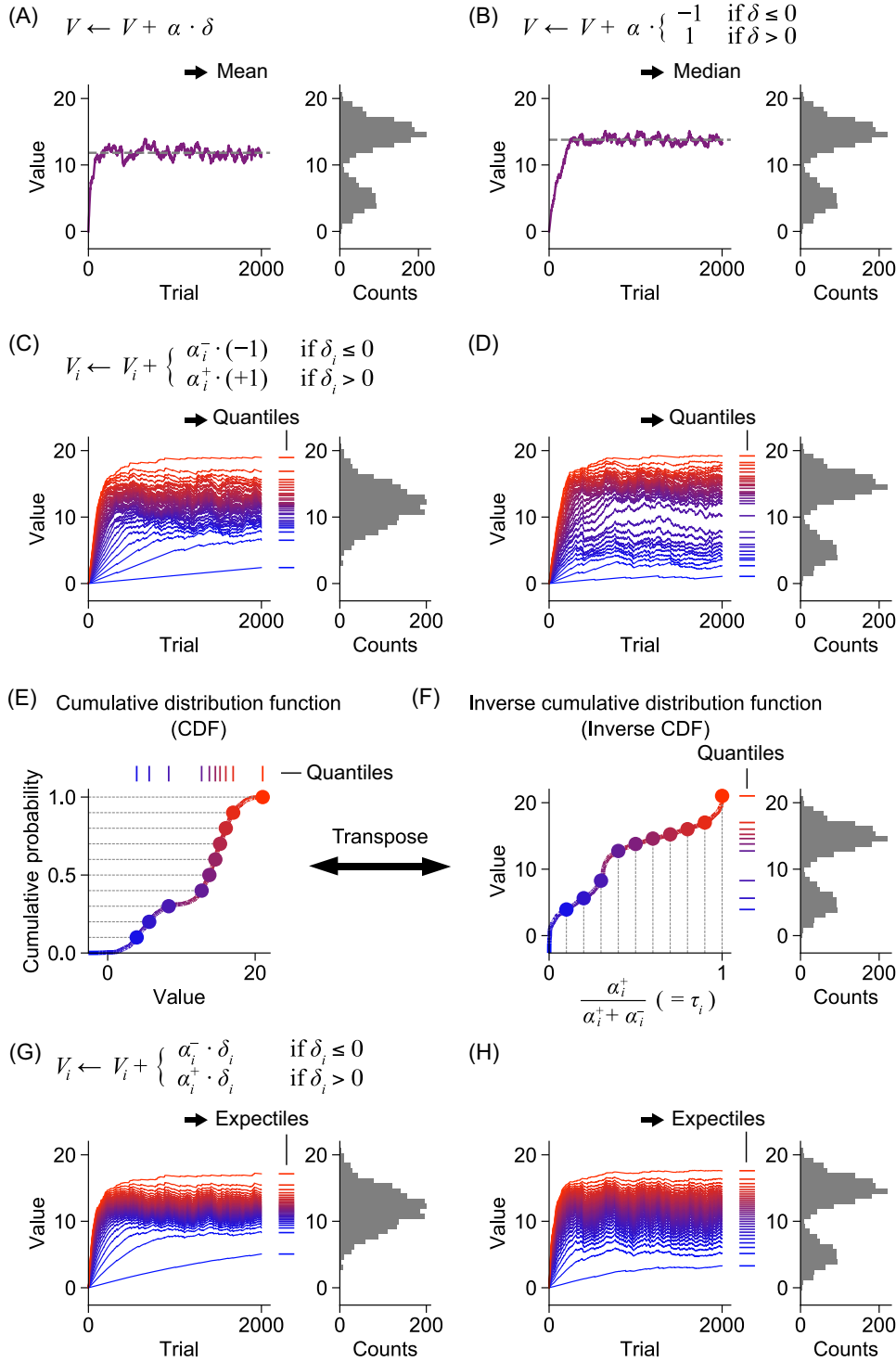


Figure 1. Deep Reinforcement Learning (RL). (A) A formulation of RL problems. In RL, an agent learns what action to take in a given state in order to maximize the cumulative sum of future rewards. In video games such as Atari games (here, the Space Invaders game is shown), an agent chooses which action $[a(t)]$, joystick turn, button press] to take based on the current state $[s(t)]$, pixel images]. The reward $[r(t)]$ is defined as the points that the agent or player earns. After David Silver's lecture slide (<https://www.davidsilver.uk/teaching/>). (B) Structure of deep Q-network (DQN). A deep artificial neural network (more specifically, a convolutional neural network) takes as input a high-dimensional state vector (in this illustration, pixel images of four consecutive Atari game frames) along with sparse scalar rewards and returns as output a vector corresponding to the value of each possible action given that state [called action values or Q-values and denoted $Q(s, a)$]. The agent chooses actions based on these Q-values. To improve performance, the original DQN implemented a technique called 'experience replay', whereby a sequence of events is stored in a memory buffer and replayed randomly during training [2]. This helped remove correlations in the observation sequence, which had previously prevented RL algorithms from being used to train neural networks. Modified from [2]. (C) Difference between traditional and distributional RL. Distributional DQN estimates a complete reward distribution for each allowable action. Modified from [6]. (D) Performance of different RL algorithms in DQN. Gray, DQN using a traditional RL algorithm [2]. Light blue, DQN using a categorical distributional RL algorithm (C51 algorithm in [6]). Blue, DQN using a distributional RL based on quantile regression [7]. Modified from [7].



Value: in the Rescorla-Wagner formulation, it is the predicted amount of reward associated with a stimulus. In the TD framework, it is the expected sum of discounted future rewards associated with a state (Box 1) or state-action combination.

Trends in Neurosciences

(See figure legend at the bottom of the next page.)

Box 1. Temporal Difference (TD) Learning

The Rescorla-Wagner (RW) rule [13], for all its success, is limited by its exclusive focus on immediate rewards. Fortunately, many of its shortcomings can be overcome by defining a different environmental structure and learning objective [9,11,12]. We start by considering arbitrary states s , which transition at each time step and sample a random reward (possibly zero or negative) from a probability distribution $R(s)$. We then define a new learning objective, the value:

$$V(s_t) := \mathbf{E}[R(s_t) + \gamma R(s_{t+1}) + \gamma^2 R(s_{t+2}) + \dots], \quad [\text{I}]$$

where $\mathbf{E}[\cdot]$ denotes an expectation over stochastic state transitions and reward emissions, and γ is a discount factor between 0 and 1, reflecting a preference for earlier rewards.

Contrary to the RW model, which cares only about the reward obtained in a trial, this model cares about (a weighted sum of) all future rewards. Since the environment is assumed to follow **Markov dynamics**, we can rewrite this relationship recursively, using the so-called Bellman equation:

$$V(s_t) := \mathbf{E}[R(s_t) + \gamma V(s_{t+1})]. \quad [\text{II}]$$

Rearranging and sampling $r_t \sim R(s_t)$ from the environment, we arrive at a new kind of RPE, namely, a TD error [4], which we also call δ to emphasize its similarity to the RPE in the RW model:

$$\delta(t) := r_t + \gamma V(s_{t+1}) - V(s_t). \quad [\text{III}]$$

The value update then occurs in exactly the same manner as before:

$$V(s_t) \leftarrow V(s_t) + \alpha \delta(t). \quad [\text{IV}]$$

The similarity between the RW and TD learning rules disguises one important difference. In the case of the RW rule, we computed the prediction error using the actual reward, R , that was experienced. In TD, we substitute R with $r_t + \gamma V(s_{t+1})$, our estimate of the target value of state s_t . But this target includes yet another value predictor $\gamma V(s_{t+1})$, which we also are trying to learn and which may in fact be inaccurate. Therefore, we use one estimate to refine a different estimate, a procedure known as ‘bootstrapping’. For that reason, unlike RW, TD learning is not a true instance of stochastic gradient descent, since changing the parameters of our value function changes not only our estimate but also our target [9]. This is the principal reason why we focus on distributional forms of the RW (rather than TD) rule in the main text. Nonetheless, and quite remarkably, this ‘bootstrapping’ procedure is proven to converge to a point near the local optimum in the case of linear function approximation [88] and can be made to work very well in practice, even in situations where theoretical convergence is not guaranteed [2].

In the case where $\alpha_i^+ > \alpha_i^-$, positive prediction errors drive learning more strongly compared with negative ones. This will cause V_i to converge to a value larger than the median, so we call such value predictors ‘optimistic’. Conversely, when $\alpha_i^+ < \alpha_i^-$, the value predictors become ‘pessimistic’. For any combination of α_i^+ and α_i^- , a value predictor that learns according to the above rule will converge to the $\frac{\alpha_i^+}{\alpha_i^+ + \alpha_i^-} = \tau_i$ -th **quantile** (Figure 2C,D). Multiple value predictors

Figure 2. Learning Rules of Distributional Reinforcement Learning: Quantile and Expectile Regression. (A) The standard Rescorla-Wagner learning rule converges to the mean of the reward distribution. (B) Modifying the update rule to use only the sign of the prediction error causes the associated value predictor to converge to the median of the reward distribution. (C,D) Adding diversity to the learning rates alongside a binarized update rule that follows the sign of the prediction error causes a family of value predictors to converge to quantiles of the reward distribution. More precisely, the value q_{τ} to which predictor i converges is the τ_i -th quantile of the distribution, where τ_i is given by $\frac{\alpha_i^+}{\alpha_i^+ + \alpha_i^-}$. This is illustrated for both unimodal (C) and bimodal (D) distributions. (E) The cumulative distribution function (CDF) is a familiar representation of a probability distribution. (F) By transposing this representation, we get the quantile function, or inverse CDF (left). Uniformly spaced quantiles cluster in regions of higher probability density (right). Together, these quantiles encode the reward distribution in a nonparametric fashion. (G,H) Multiplying the prediction error by asymmetric learning rates yields expectiles. Relative to quantiles, expectiles are pulled toward the mean for both unimodal (G) and bimodal (H) distributions. Abbreviations: α , learning rate; δ , reward prediction error; V , predicted value.

associated with different τ s thus form a **population code** that is the inverse of the cumulative distribution function (CDF) (Figure 2E,F) of rewards.

One can also consider a family of value predictors that retains the original form of the update rule in Equation 1, such that

$$V_i \leftarrow V_i + \begin{cases} \alpha_i^- \cdot \delta_i & \text{if } \delta_i \leq 0 \\ \alpha_i^+ \cdot \delta_i & \text{if } \delta_i > 0 \end{cases} \quad [4]$$

This update rule gives rise to a range of value estimates called **expectiles** (Figure 2G,H), which generalize the mean just as quantiles generalize the median. However, unlike quantiles, expectiles do not bear a straightforward relationship to the CDF. To understand them, it is necessary to adopt a more general perspective on learning.

Distributional RL as the Process of Minimizing Estimation Errors

The distributional RL algorithms illustrated earlier are known as quantile and expectile regression [7,8]. This is because in addition to thinking of quantiles as places to divide ordered samples into two sets of given size ratios, they can be derived from the perspective of minimizing certain continuous **loss functions**, which is precisely what a regression does [15,16]. We will demonstrate this here by re-deriving the aforementioned learning algorithms for quantiles and expectiles from the common perspective of regression (Figure 3A).

Let us first consider the most widespread error measure used in linear regression, the mean squared error (MSE), in the context of learning about rewards (r). Assuming that we have observed rewards r_1, r_2, \dots, r_N across N trials, the MSE of some value V is defined as

$$MSE(V) = \frac{1}{N} \sum_{n=1}^N (r_n - V)^2 \quad [5]$$

and so measures the squared difference of this value to each observed reward, averaged across all rewards [17]. This definition makes the MSE a function of V , such that as the value of V changes, the MSE will increase or decrease (Figure 3B). The question we would like to address is: what is the V that minimizes the MSE? To find this minimum, we set the derivative of the MSE with respect to V to zero and solve for V , resulting in $V = \frac{1}{N} \sum_{n=1}^N r_n$. Therefore, if one defines the prediction error associated with the n th reward as $\delta_n = r_n - V$, then the MSE (the mean across all δ_n^2) is minimized if V equals the average reward across trials.

One approach to minimize Equation 5 is to memorize all rewards across trials and subsequently compute their mean. However, once the number of trials N is large, this method is neither memory-efficient nor biologically plausible. An alternative method that is widely applied in machine learning is **stochastic gradient descent** [18]. Revisiting the earlier example, assume that the rewards r_1, r_2, \dots, r_N are observed one after the other. We would like to find a local learning rule that converges on an estimate V that approximately minimizes the sum of squared prediction errors.

With stochastic gradient descent, the current reward estimate V is adjusted every time a new observation r_n becomes available by moving one small step down along the **gradient** of the

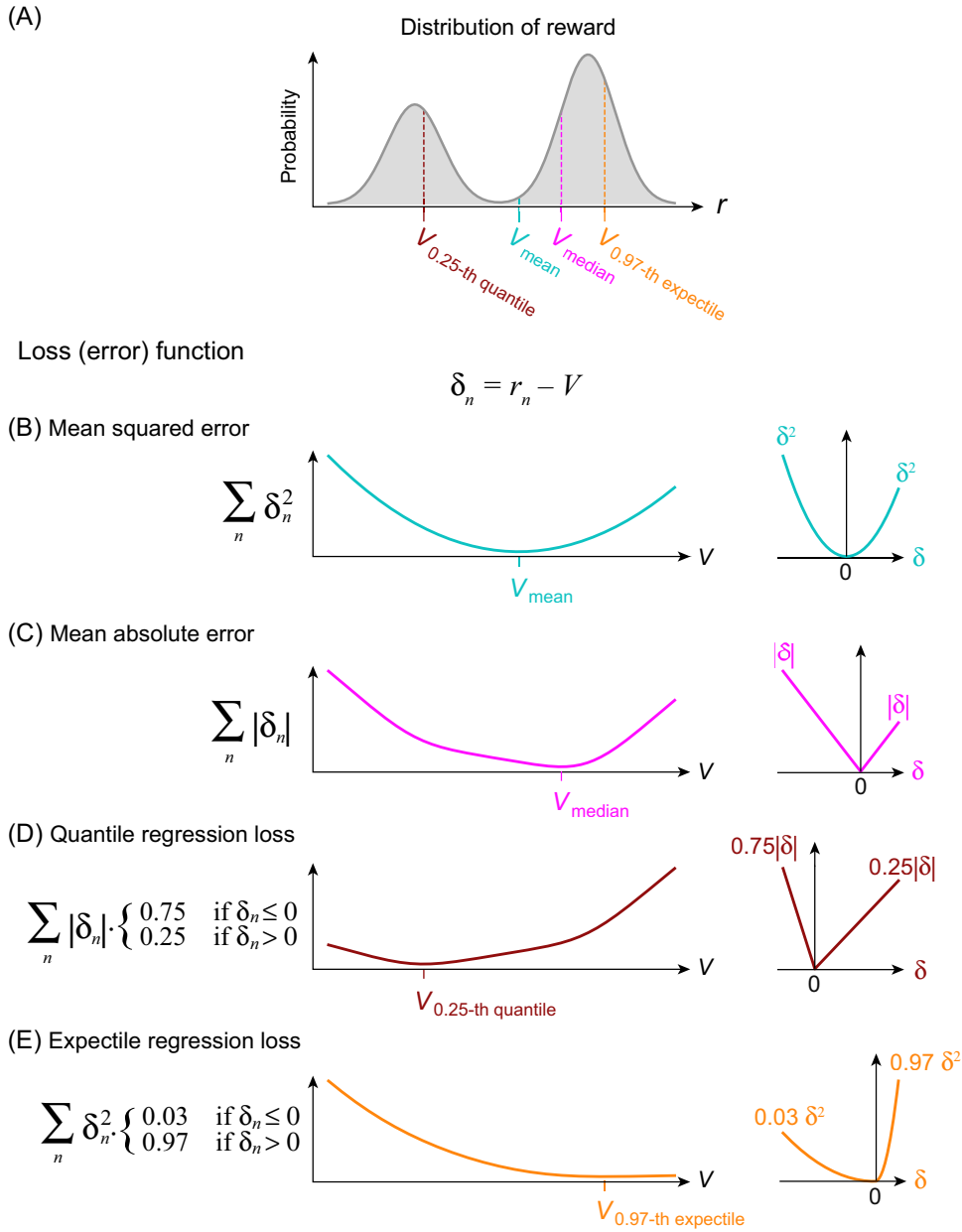


Figure 3. Distributional Reinforcement Learning as Minimizing a Loss Function. (A) The reward (r) probabilities of an example reward distribution. Mean V_{mean} , median V_{median} , 0.25-quantile $V_{0.25\text{-quantile}}$, and 0.97-expectile $V_{0.97\text{-expectile}}$ of this distribution are indicated with different colors. (B–E) Loss as a function of the value estimate V (left) when the rewards follow the distribution presented in (A), illustrating that $V = V_{\text{mean}}$ minimizes the mean squared error (B), $V = V_{\text{median}}$ minimizes the mean absolute error (C), $V = V_{0.25\text{-quantile}}$ minimizes the quantile regression loss for $\tau = 0.25$ (D), and $V = V_{0.97\text{-expectile}}$ minimizes the expectile regression loss for $\tau = 0.97$ (E). The right panels show the loss on a single sample as a function of the reward prediction error δ .

squared error. [For mathematical convenience, here we actually compute the gradient of half the squared error, $\nabla(\delta_n^2/2)$, but the conceptual approach is the same.] This gradient measures how the output of the loss function associated with this new observation, δ_n^2 , will change when the

relevant parameters are modified. In this case, the relevant parameter is just V , such that the required gradient is given by the derivative of $\delta_n^2/2$ with respect to V :

$$\begin{aligned}\nabla(\delta_n^2/2) &= \frac{d(r_n - V)^2/2}{dV} \\ &= -(r_n - V) \\ &= -\delta_n.\end{aligned}\quad [6]$$

The parameter V will then be updated according to $V \leftarrow V - \alpha \nabla(\delta_n^2/2)$. After substituting the gradient, we obtain

$$V \leftarrow V + \alpha \cdot \delta_n. \quad [7]$$

The current error function, which depends only on the most recently available reward r_n , here acts as a proxy of the error function encompassing all trials, Equation 6. Intuitively speaking, subtracting α times the gradient from the current reward estimate, as performed in Equation 7, corresponds to adjusting the reward estimate slightly towards the steepest drop of the current error function. Notice that Equation 7 is equivalent to Equation 1. Therefore, the RW rule is equivalent to stochastic gradient descent if we measure the loss by the MSE [19].

In general, as long as the error we aim to minimize has a form similar to Equation 5, in which the global error is a sum of local errors, each of which only depends on the reward in one trial, we can always apply an update rule similar to Equation 7, using the corresponding gradient to carry out stochastic gradient descent. Below, we apply this approach to a variety of loss functions to derive the corresponding update rules.

One simple change is to replace the square of δ_n by its absolute value, leading to the mean absolute error

$$\frac{1}{N} \sum_{n=1}^N |\delta_n|. \quad [8]$$

In this case, the derivative with respect to V of $|\delta_n| = |r_n - V|$ is simply $-\text{sign}(\delta_n)$, which readers will recognize as the update that converges to the median of the reward distribution (Figure 3C).

If we additionally weigh positive and negative errors differently,

$$\frac{1}{N} \sum_{n=1}^N |\delta_n| \cdot \begin{cases} 1 - \tau & \text{if } \delta_n \leq 0 \\ \tau & \text{if } \delta_n > 0 \end{cases} \quad [9]$$

where τ is a fixed value between 0 and 1, the best estimate becomes the τ -th quantile of the reward distribution [16]. Hence, Equation 9 is called the quantile regression loss function.

We can again turn the global error function, Equation 9, into a sequential update by stochastic gradient descent, resulting in

$$V \leftarrow V + \alpha \cdot \begin{cases} -(1 - \tau) & \text{if } \delta_n \leq 0 \\ \tau & \text{if } \delta_n > 0 \end{cases} \quad [10]$$

If δ_n is negative, the rate parameter equals $-\alpha(1 - \tau) = -\alpha^-$; if it is positive, this product becomes $\alpha\tau = \alpha^+$. This confirms the intuition developed in the preceding section (Equation 3), showing that such an update rule indeed minimizes the quantile regression loss function and approximates the τ -th quantile (Figure 3D).

To arrive at expectile regression, we move one step further and replace the absolute value of δ_n with its square in Equation 9. This yields the weighted squared error loss function, also called the expectile regression loss function [15,20],

$$\frac{1}{N} \sum_{n=1}^N \delta_n^2 \cdot \begin{cases} 1 - \tau & \text{if } \delta_n \leq 0 \\ \tau & \text{if } \delta_n > 0 \end{cases} \quad [11]$$

whose associated best estimate is the τ -th expectile (Figure 3E). For $\tau = 0.5$, the two weights are equal, such that the error measure becomes equivalent to (half) the MSE, Equation 1. This confirms that the 0.5-th expectile is the mean across all rewards. Other expectiles can be interpreted as the analogue to quantiles, but for squared rather than absolute errors.

Stochastic gradient descent on Equation 11 results in the update rule

$$V \leftarrow V + \alpha \delta_n \cdot \begin{cases} 1 - \tau & \text{if } \delta_n \leq 0 \\ \tau & \text{if } \delta_n > 0 \end{cases} \quad [12]$$

which is a modified version of RW rule in which the rate parameter takes on different values for negative and positive δ_n (Equation 4).

Different loss functions therefore lead to estimating different statistics of the reward distribution. Even if we fix a loss function, however, there are still many possible ways to represent and learn the corresponding statistic. For instance, instead of storing the estimated quantiles directly and performing updates on them as in Equation 10, the brain may approximate quantiles by a parametric vector-valued function $\mathbf{q}(\boldsymbol{\theta}) = (q_1(\boldsymbol{\theta}), \dots, q_M(\boldsymbol{\theta}))$, with parameters $\boldsymbol{\theta}$ that might correspond to synaptic strengths between different neurons and outputs q_i denoting the value of the τ_i -th quantile (\mathbf{q} and $\boldsymbol{\theta}$ are vectors and thus bold). The same strategy could also apply to expectiles $\mathbf{e}(\boldsymbol{\theta})$.

To find the update rules for these representations, we can again use stochastic gradient descent. However, rather than computing the gradient with respect to V , we now compute it with respect to the function's parameters, $\boldsymbol{\theta}$. Following similar calculations as shown earlier, this update rule for learning quantiles turns out to be

$$\boldsymbol{\theta} \leftarrow \boldsymbol{\theta} + \alpha \sum_{i=1}^M \nabla_{\boldsymbol{\theta}} q_i(\boldsymbol{\theta}) \cdot \begin{cases} -(1 - \tau) & \text{if } \delta_{i,n} \leq 0 \\ \tau & \text{if } \delta_{i,n} > 0 \end{cases} \quad [13]$$

while for learning expectiles, it becomes

$$\boldsymbol{\theta} \leftarrow \boldsymbol{\theta} + \alpha \sum_{i=1}^M \delta_{i,n} \nabla_{\boldsymbol{\theta}} e_i(\boldsymbol{\theta}) \cdot \begin{cases} 1 - \tau & \text{if } \delta_{i,n} \leq 0 \\ \tau & \text{if } \delta_{i,n} > 0 \end{cases} \quad [14]$$

Thus, the only changes to the update rules are: (i) the addition of the gradient terms $\nabla_{\boldsymbol{\theta}} q_i(\boldsymbol{\theta})$ or $\nabla_{\boldsymbol{\theta}} e_i(\boldsymbol{\theta})$, and (ii) the sum of contributions from different component quantiles or expectiles. For

components $q_i(\theta)$ or $e_i(\theta)$ estimated as linear parametric functions $\mathbf{u}_i^T \theta + v_i$, this gradient is \mathbf{u}_i , which results in a simple rescaling of the parameter update by \mathbf{u}_i . Such functions include single-layer neural networks, in which case it is synaptic weights that are incremented or decremented. If we move from linear to nonlinear parametric functions, like multilayer neural networks, the gradients (and therefore the updates) become slightly more complex, but the general principles of stochastic gradient descent remain. In sum, by treating distributional RL as a regression problem and performing stochastic gradient descent on an appropriate loss function, one can easily derive update rules that converge to the desired statistics of the reward distribution under a wide variety of parameterizations.

Traditional and Distributional RL in the Brain

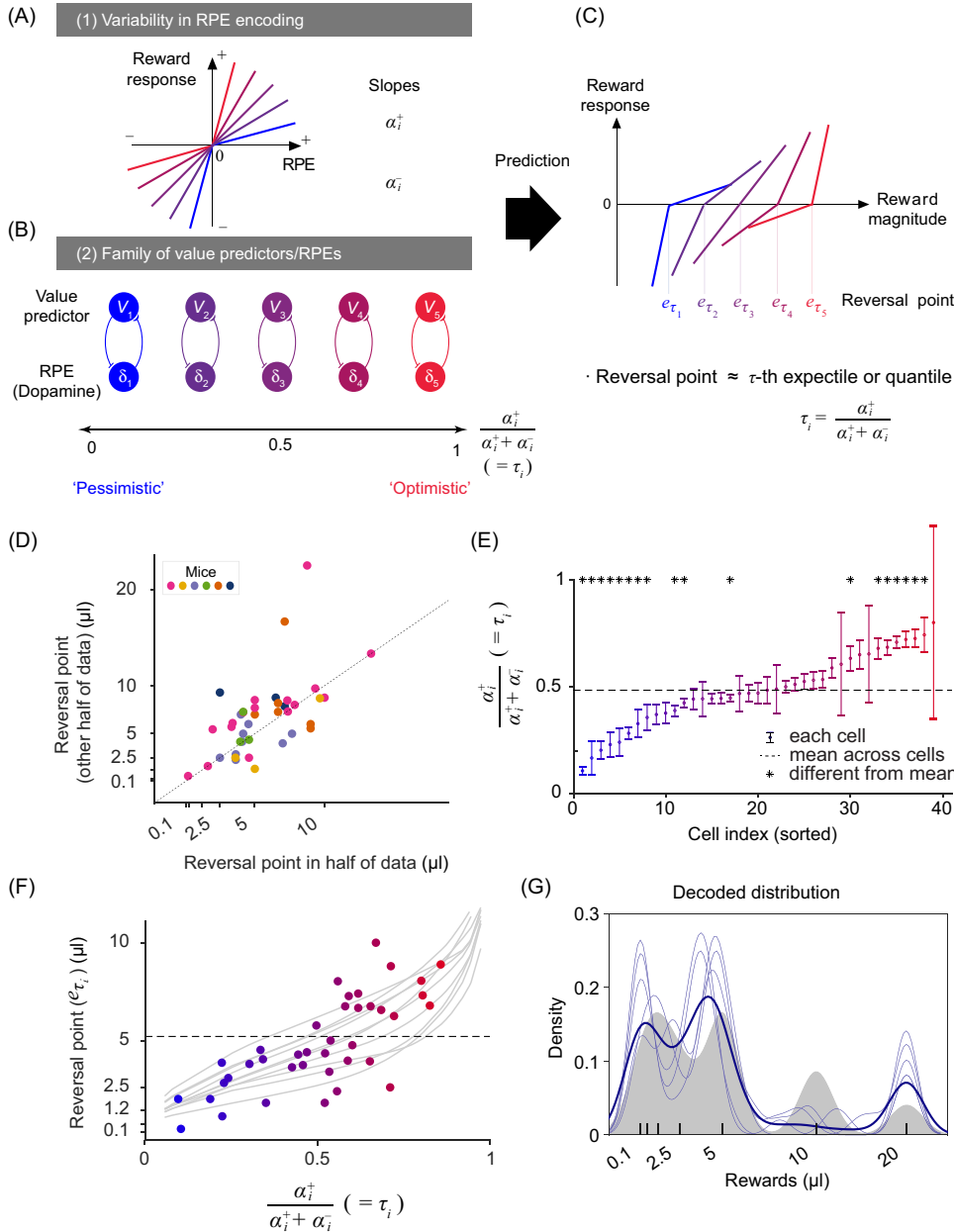
The idea that the brain uses some form of RL to select appropriate actions has been supported by a number of observations of animal behavior and neuronal activity [12,13,21–23]. One of the strongest pieces of evidence is the close relationship between the activity of dopamine neurons and the reward prediction error (RPE) term in RL algorithms [21–23]. Neural activity representing value, the other critical variable in these algorithms, is also found in dopamine-recipient areas [24–26].

In mammals, dopamine neurons are located mainly in the ventral tegmental area (VTA) and substantia nigra pars compacta in the midbrain, from which they send long axons to a wide swath of the brain that includes the striatum, prefrontal cortex, and amygdala. The information conveyed by different dopamine neurons varies greatly based on their projection targets [27–30], with the dopamine neurons in the VTA that project to the ventral part of the striatum (nucleus accumbens) thought to mainly signal RPEs (but see [31,32]). Beyond this coarse projection specificity, which has been reviewed elsewhere [27,28], there is also fine-grained diversity within VTA dopamine neurons, which is our focus here. While the activity of these neurons appears quite homogenous compared with neurons in other parts of the brain [33,34], recent studies have revealed more diverse firing patterns [35], at least some of which may reflect systematic variation in RPE signals [36]. Distributional RL offers one possible explanation for the functional significance of this diversity within the VTA.

Empirically Testing Distributional RL

The key ingredient that transforms traditional RL into distributional RL is the diversity in learning rate parameters for positive and negative RPEs (α^+ and α^-), or, more critically, the ratio between them, $\tau = \frac{\alpha^+}{\alpha^+ + \alpha^-}$, which we call the asymmetric scaling factor [7,8]. Although the biological processes that implement α^+ and α^- remain unclear, one possibility is that these parameters correspond to how the firing of each dopamine neuron scales up or down with respect to positive or negative RPEs, respectively. This leads to several testable predictions in the expectile setting.

First, there should be ample diversity in asymmetric scaling factors across dopamine neurons (Figure 4A), which should result in optimistic and pessimistic value predictors (Figure 4B). The information contained in these value predictors (V_i), in turn, is routed back to dopamine neurons for computing RPEs, subtracting ‘expectation’ (V_i) from the response to a received reward (R). This means that for optimistic dopamine neurons, which are coupled to relatively high value predictors, larger rewards are necessary to cancel out their reward response and obtain zero RPE. Thus, optimistic dopamine neurons with $\alpha^+ > \alpha^-$ will have ‘reversal points’ that are shifted towards above-average reward magnitudes (Figure 4C). Conversely, pessimistic dopamine neurons with $\alpha^+ < \alpha^-$ will have reversal points shifted towards below-average reward magnitudes. Across the population of neurons, distributional RL therefore makes the unique prediction that the reversal points of dopamine response functions should be positively correlated with their asymmetric scaling factors $\left(\tau = \frac{\alpha^+}{\alpha^+ + \alpha^-} \right)$.



Trends in Neurosciences

Figure 4. The Structured Diversity of Midbrain Dopamine Neurons Is Consistent with Distributional Reinforcement Learning. (A) Schematic of five different response functions (spiking activity of dopamine neurons) to positive and negative reward prediction errors (RPEs). In this model, the slope of the response function to positive and negative RPEs corresponds to the learning rates α^+ and α^- . Diversity in α^+ and α^- values results in different asymmetric scaling factors $\left(\frac{\alpha_i^+}{\alpha_i^+ + \alpha_i^-}\right)$. (B) RPE channels (δ) with $\alpha^+ < \alpha^-$ overweight negative prediction errors, resulting in pessimistic (blue) value predictors (V), while RPE channels with $\alpha^+ > \alpha^-$ overweight positive prediction errors and result in optimistic (red) value predictors. This representation corresponds to the Rescorla-Wagner approach in which RPE and value pairs form separate channels, with no crosstalk between channels with different scaling factors. See [Box 2](#) for the general update rule when this condition is not met. (C) Given that different value predictors encode different reward magnitudes, the corresponding RPE channels will have diverse reversal points (reward magnitudes that elicit no RPE

(Figure legend continued at the bottom of the next page.)

A recent study [8] tested these predictions using existing data from optogenetically tagged VTA dopamine neurons in mice performing a task in which a single odor preceded a variable reward [34,37]. Responses differed in subtle but important ways among dopamine neurons; some neurons were consistently excited, even for below-average rewards, while others were excited only by rewards that exceeded the average (Figure 4D) [8]. The reversal points in this task were assumed to reflect different value predictions: each reversal point e_{τ_i} was interpreted as the τ_i -th expectile of the reward distribution.

To independently compute τ_i , α_i^+ and α_i^- were estimated for each neuron i as the slopes of the average response function above and below the neuron's reversal point. This analysis revealed significant variability in asymmetric scaling factors, tiling a relatively wide range between 0 and 1 (Figure 4E). Critically, these asymmetric scaling factors were positively correlated with the reversal points, as predicted earlier (Figure 4F). Finally, such structured heterogeneity in dopamine neurons allowed the authors to decode possible reward distributions from the neural data by finding reward distributions compatible with the expectiles defined by $\{\tau_i, e_{\tau_i}\}$ (Figure 4G). Importantly, this decoding procedure strongly relied on the structured heterogeneity assumption imposed by an expectile code and should have been unsuccessful if the variability merely reflected random noise.

Distributional RL lends itself to several additional experimental predictions, which remain to be tested [8]. For example, dopamine neurons should show consistent asymmetric scaling factors across different reward distributions. Furthermore, optimistic cells should learn more slowly from negative prediction errors compared with pessimistic cells and therefore be slower to devalue when reward contingencies are changed. Quantile-like distributions of value should be present in both the downstream targets as well as the inputs to VTA dopamine neurons [8], with optimistic neurons in one region projecting predominantly to optimistic neurons elsewhere. Finally, distributional representations should predict behavior in operant tasks, such that biasing dopamine neurons optimistically [38] elicits risk-seeking behavior.

Is Distributional RL Biologically Plausible?

The studies discussed earlier are promising, but the prospect of distributional RL in the brain raises many new questions regarding development, plasticity, and computation in the dopamine system.

Diversity in Asymmetric Scaling and Independent Loops

The critical feature of distributional RL, the diversity of asymmetric scaling factors in dopamine signals (Figure 4A), might be established developmentally simply through stochasticity in wiring. However, there may be more specific mechanisms in place to ensure such diversity. Recent evidence suggests that positive and negative RPEs may be shaped by relatively separate mechanisms. For example, lesions of the lateral habenula or rostromedial tegmental nucleus (RMTg)

activity relative to baseline). The reversal points correspond to the values V_i of the τ_i -th expectiles of the reward distribution. (D) Reversal points of optotagged dopamine neurons are consistent across two independent sets of trials, suggesting that the diversity observed is reliable ($P = 1.8 \times 10^{-5}$, each point represents a cell). Modified from [8]. (E) Diversity in asymmetric scaling in dopamine neurons tiles the entire [0, 1] interval and is statistically reliable [one-way ANOVA; $F(38, 234) = 2.93$, $P = 4 \times 10^{-7}$]. Modified from [8]. (F) Significant correlation between reversal points and asymmetric scaling in dopamine neurons (each point is a cell, linear regression $P = 8.1 \times 10^{-5}$). Gray traces show variability over distributional RL simulations run to calculate reversal points in this task. Modified from [8]. (G) Decoding of the reward distribution from dopamine cell activity using an expectile code. The expectiles of the distribution, $\{\tau_i, e_{\tau_i}\}$, were defined by the asymmetries and reversal points of dopamine neurons, respectively. Gray area represents the smoothed reward distribution, light blue traces represent several decoding runs, and the dark blue trace represents their mean. Modified from [8].

result in a preferential reduction of responses to negative RPEs [38,39]. Intriguingly, habenula-lesioned animals become 'optimistic' in reward-seeking behavior as well [38], raising the possibility that asymmetric scaling factors might influence behavior.

One important assumption in the distributional RL model discussed earlier is the independence between loops of dopamine neuron-value predictor pairs, to separate optimistic and pessimistic value predictors (Figure 4B). Of course, complete independence of these loops would be unrealistic, given the complexity of wiring in the brain. Axons of dopamine neurons branch extensively in the dorsal striatum, but branching in the ventral striatum is much more restricted [40–42]. It turns out that adding relatively extensive crosstalk between neighboring dopamine projections does not disturb distributional RL [8], provided that optimistic and pessimistic dopamine neurons (and value predictors) are topographically organized (e.g., [42]). One way to create such a gradient would be through inhomogeneous projections of inputs generating excitatory and inhibitory responses in dopamine neurons, as is the case for input from RMTg [43,44]. There is additional topographic variability in the intrinsic membrane properties of dopamine neurons, particularly in their response to hyperpolarizing current, that is hypothesized to render them differentially sensitive to positive and negative RPEs [45], adding yet another layer of diversity that could support distributional RL.

Learning Rate Parameters in Striatum and Cortex

Up to this point, we have assumed that asymmetric scaling factors are already implemented in the firing of dopamine neurons [8]. However, learning rate parameters may also be affected by downstream processes such as synaptic plasticity at dopamine-recipient neurons. Recent studies have begun to establish experimental paradigms for inducing synaptic plasticity using transient dopamine release *in vitro* and measuring the resulting 'plasticity function' [46,47]. Along these lines, recent studies indicate that positive and negative RPEs are processed differently, depending on whether the target cells in the striatum express D1- or D2-type dopamine receptors [46,47]. This dichotomous circuit architecture resembles the binarized update rules shown earlier, but it is at present unclear whether it enables distributional RL in the brain.

Normative models predict that the overall learning rate should be dynamically modulated by the volatility of rewards in the environment [48]. The mechanism of distributional RL leaves open the possibility that additional, extrinsic factors might modulate the overall learning rate, or 'gain', while leaving the ratio between positive and negative learning rates, and thus the distributional codes, relatively unchanged. Neuromodulators such as serotonin and norepinephrine, acting in cortical or striatal areas, are good candidates for tuning such a gain mechanism [49,50]. Furthermore, frontal regions such as the anterior cingulate [48,51] and orbitofrontal cortex [52], which project densely to more ventral portions of the striatum [53], also encode value, prediction error, uncertainty, and volatility and have been hypothesized to adjust the gain under conditions of uncertainty [54]. In principle, this additional, cortical level of regulation could go beyond adapting the learning rate to directly influencing the computation or readout of a quantile-like code, for example, by biasing downstream circuits towards more optimistic or pessimistic value predictors.

The importance of interplay between cortical and subcortical circuits in this context is highlighted by the Iowa Gambling Task (IGT), which was originally designed to characterize deficits in risk-based decision-making in patients with orbitofrontal damage [55]. Parkinson's patients treated with L-DOPA, which elevates dopamine levels (but not unmedicated patients [56], who have normal levels of ventral striatal dopamine [57]) also exhibit deficits in the IGT, as well as impulse control disorders such as pathological gambling [58,59]. This pattern suggests that L-DOPA may compromise the fidelity of distributional RL and is consistent with previous reports that

dopaminergic [60] and ventral striatal [61,62] activity can combine information about reward mean and variance to influence choice behavior [63–66]. Distributional RL provides a new potential mechanism to explain the involvement of dopaminergic activity in risk and could play a critical role in guiding efficient exploration of uncertain environments [67].

How Does the Brain Benefit from Distributional Representations?

The performance improvement garnered by distributional RL in previous studies [6–8,10] is not due to better decision-making at the action selection stage; the modified DQN in these studies computed the mean of the inferred reward distribution to decide which action to take. Instead, it is thought that the benefit of distributional RL comes mainly from its ability to support efficient representation learning in multilayer neural networks. In traditional DQN, states with the same expected value yield the same output even if they give rise to very different reward distributions; thus, there is no drive to distinguish these states in lower layers of the network. A distributional DQN, by contrast, outputs the complete return distribution and so requires distinct representations in the hidden layers [8]. By combining the quantile or expectile loss with backpropagation or other optimization methods, deep neural networks can convey this much richer information to lower layers and thereby improve performance even with risk-neutral policies. Linear function approximators (e.g., single-layer neural networks) do not learn hidden representations, so distributional RL confers no benefit for estimating the expected value in the linear setting [68]. Whether or not such distributional codes also promote state learning in the brain remains to be tested experimentally. However, it is compelling to speculate that such codes are central not just for learning distributions of reward magnitude [8,34,69] and probability [38], but also for tracking rewards across uncertain delay intervals [70–72] and representing such distributions in the common currency of value.

Quantile-like codes are **nonparametric codes**, as they do not *a priori* assume a specific form of a probability distribution with associated parameters. Previous studies have proposed different population coding schemes. For example, probabilistic population codes (PPCs) [73,74] and distributed distributional codes (DDCs) [75,76] employ population coding schemes from which various statistical parameters of a distribution can be read out, making them **parametric codes**. As a simple example, a PPC might encode a Gaussian distribution, in which case the mean would be reflected in which specific neurons are most active and the variance would be reflected in the inverse of the overall activity [73]. It is not yet known whether parametric codes predict similar structured heterogeneity of dopamine neuron RPEs. Understanding the precise format of population codes is crucial because it helps determine how downstream neurons can use that information to guide behavior. While PPCs, for example, support Bayesian inference [73,77], quantile codes could support simple implementations [8] of cumulative prospect theory [78], which provides a descriptive model of human and animal behavior [79]. There have also been simpler algorithms proposed that learn a specific parameter (e.g., variance) of a distribution [54,80]. While these algorithms are not meant to learn the entire shape of a distribution, such parameters may be useful for specific purposes, and it will be important to clarify under what circumstances quantile-like codes outperform these simpler mechanisms.

Once an agent has sufficient experience, the full distribution of future returns captures intrinsic and irreducible stochasticity in the environment, such as variability in reward size. However, there are several additional possible sources of uncertainty in the RL framework, such as state, value, and policy uncertainty, all of which have been proposed to affect dopamine cell activity, albeit through different mechanisms [81]. For example, there is strong evidence that reward expectations inferred from ambiguous state information [71,72,82] or perceptual uncertainty [83,84] modulate dopamine activity. Future avenues of research should explore how a

distributional representation of outcomes can be combined with such independent forms of uncertainty to produce more robust learning.

Distributional TD Updates in the Brain

A subtle but crucial distinction between traditional and distributional RL when moving from the RW to the TD framework centers on the computation of the prediction error δ (Box 2). In the case of traditional RL, δ can be computed from a single, local estimate of the value at the succeeding state. By contrast, distributional RL often requires samples to be generated from the reward distribution of the succeeding state in order to compute δ [7,8]. The information required to generate these samples is no longer contained locally within a (hypothetical) single unit; instead, it is distributed across a population of neurons and hence available only globally.

Box 2. Distributional Temporal Difference (TD) Learning

In distributional TD learning, the objective is no longer simply the expected value, but rather the entire distribution over cumulative discounted future reward beginning in state s_t . This is called the return distribution and denoted $Z(s_t)$ [6]. We emphasize that $Z(s_t)$ is a random variable, unlike its expectation $V(s_t) = \mathbf{E}[Z(s_t)]$. Nonetheless, we can write down a similar ‘distributional Bellman equation’, where the D denotes equality of distribution:

$$Z(s_t) \stackrel{D}{=} R(s_t) + \gamma Z(s_{t+1}). \quad [\text{I}]$$

If we were to take the expectation on both sides, we would get back our familiar, nondistributional Bellman equation. In contrast, we now seek to learn each statistic $V(s_t)$ that minimizes the quantile regression loss (Equation 9 in the main text) on samples from $Z(s_t)$ for $\tau = \tau_t$. One way to do this is by computing samples of the distributional TD error [7]:

$$\tilde{\delta}_t(t) := r_t + \gamma \tilde{z}(s_{t+1}) - V_t(s_t). \quad [\text{II}]$$

Here, r_t is a sample from $R(s_t)$, provided by the environment, and $\tilde{z}(s_{t+1})$ is a sample from the estimated distribution $Z(s_{t+1})$. Note that this TD error departs from the traditional form; in particular, as $\tilde{z}(s_{t+1})$ is fundamentally random, so is the TD error, and $\tilde{\delta}_t(t) \neq r_t + \gamma V(s_{t+1}) - V(s_t)$, as one might otherwise expect. Furthermore, since $\tilde{\delta}_t(t)$ enters the value update equations in a nonlinear way, we cannot simply operate with the average TD error, $\mathbf{E}[\tilde{\delta}_t(t)]$. Despite these differences, our value predictors can be updated in direct analogy to the distributional RW rule:

$$V_i(s_t) \leftarrow V_i(s_t) + \begin{cases} \alpha_i^- \cdot (-1) & \text{if } \tilde{\delta}_i(t) \leq 0 \\ \alpha_i^+ \cdot (+1) & \text{if } \tilde{\delta}_i(t) > 0 \end{cases} \quad [\text{III}]$$

While asymptotically correct, a strategy that relies on a single sample $\tilde{z}(s_{t+1})$ from the upcoming reward distribution, and associated single $\tilde{\delta}_i(t)$ sample, would be limited by high variance. To reduce variance, we average across J updates, each of which depends on its own sample of $\tilde{\delta}_i(t)$ [7]:

$$\mathbf{E}[\Delta V_i(s_t)] = \frac{1}{J} \sum_{j=1}^J \begin{cases} \alpha_i^- \cdot (-1) & \text{if } \tilde{\delta}_{i,j}(t) \leq 0 \\ \alpha_i^+ \cdot (+1) & \text{if } \tilde{\delta}_{i,j}(t) > 0 \end{cases} \quad [\text{IV}]$$

$$V_i(s_t) \leftarrow V_i(s_t) + \mathbf{E}[\Delta V_i(s_t)]. \quad [\text{V}]$$

The expected update (Equation V) becomes equivalent to the sample update (Equation III) when $Z(s_{t+1})$ collapses to a single Dirac, in which case all $\tilde{z}(s_{t+1})$ are equivalent, and to the RW quantile update (Equation 3 in the main text) when no future reward is expected, in which case all $\tilde{z}(s_{t+1})$ are zero. This last case is the regime explored in work to date [8] and in most of the present article, for simplicity.

Computing $\mathbf{E}[\Delta V_i(s_t)]$ (Equation IV) is straightforward for quantiles, since quantiles with uniformly spaced τ_i can be treated as samples from the underlying distribution as long as the number of quantiles is reasonably large. We can therefore simply interpret each quantile $V_j(s_{t+1})$ as a sample from $Z(s_{t+1})$ and compute the expectation of $\Delta V_i(s_t)$ over j for all pairs of $(V_i(s_t), V_j(s_{t+1}))$ [7]. However, performing similar sampling for a given set of discrete expectiles requires a different and currently computationally expensive approach [89]. It remains to be seen whether alternative sampling strategies, or other approximations not dependent on sampling, can be implemented to ensure robust, efficient computation of these estimators in a biologically plausible manner.

Computing δ in the general TD case thus requires more elaborate feedback than simple TD-value predictor loops (Box 2). Future work should seek to identify neural architectures that could compute the distributional TD update, as well as experimental paradigms or environments that demand such an update.

Concluding Remarks

Distributional RL arises from structured diversity in RPEs. The specific type of diversity confers a computational advantage, providing a normative perspective on the diversity of dopamine neuron firing. It is interesting to note that the signatures of this type of diversity were present in previous studies, but were typically averaged out to focus on general trends across dopamine neurons [34,69,85]. This attests to the potential of machine learning to inform the study of the brain: without the development of distributional RL, this type of neural variability might have been discarded as mere ‘noise’.

Beyond the dopamine system, the efficacy of quantile-like codes in deep RL and the biological plausibility of the associated learning rules raise new possibilities for neural coding. Whether such codes exist elsewhere in the brain, and how they interact with other population coding schemes, remains unknown (see Outstanding Questions). Generally, the optimal type and format of a neural code depends on the specific computations that it facilitates. Artificial neural networks specifically adapted for performance on machine learning tasks may reveal novel combinations of neural codes and related computations, as has been widely documented in the primate visual system [86,87]. Ongoing collaborations in this area will help close the loop between biological and artificial neural networks and push the frontiers of neuroscience and AI.

Acknowledgments

We thank Sandra Romero Pinto, John Mikhael, Isobel Green, Johannes Bill, and Emma Krause for comments on the manuscript. Sara Matias is supported by the Human Frontier Science Program (LT000801/2018). We thank Will Dabney, Zeb Kurth-Nelson, and Matthew Botvinick for discussion. Our research related to the subject discussed here has been supported by a National Institutes of Health BRAIN Initiative grant (R01 NS116753).

References

- LeCun, Y. et al. (2015) Deep learning. *Nature* 521, 436–444
- Mnih, V. et al. (2015) Human-level control through deep reinforcement learning. *Nature* 518, 529–533
- Silver, D. et al. (2016) Mastering the game of Go with deep neural networks and tree search. *Nature* 529, 484–489
- Botvinick, M. et al. (2019) Reinforcement learning, fast and slow. *Trends Cogn. Sci. (Regul. Ed.)* 23, 408–422
- Hassabis, D. et al. (2017) Neuroscience-inspired artificial intelligence. *Neuron* 95, 245–258
- Bellemare, M.G. et al. (2017) A distributional perspective on reinforcement learning. In *Proceedings of the 34th International Conference on Machine Learning - Volume 70*
- Dabney, W. et al. (2018) Distributional reinforcement learning with quantile regression. In *Proceedings in Thirty-Second AAAI Conference on Artificial Intelligence*
- Dabney, W. et al. (2020) A distributional code for value in dopamine-based reinforcement learning. *Nature* 577, 671–675
- Sutton, R.S. and Barto, A.G. (1998) *Reinforcement Learning: An Introduction*, MIT Press
- Hessel, M. et al. (2018) Rainbow: combining improvements in deep reinforcement learning. In *The Thirty-second AAAI Conference on Artificial Intelligence*, pp. 3215–3222
- Sutton, R.S. (1988) Learning to predict by the methods of temporal differences. *Mach. Learn.* 3, 9–44
- Sutton, R.S. and Barto, A.G. (1990) Time-derivative models of Pavlovian reinforcement. In *Learning and Computational Neuroscience: Foundations of Adaptive Networks* (Gabriel, M. and Moore, J., eds), pp. 497–537, MIT Press
- Rescorla, R.A. and Wagner, A.R. (1972) A theory of Pavlovian conditioning: variations in the effectiveness of reinforcement and nonreinforcement. In *Classical Conditioning II: Current Research and Theory* (Black, A. and Prokasy, W., eds), pp. 64–99, Appleton-Century-Crofts
- Yamada, H. et al. (2013) Thirst-dependent risk preferences in monkeys identify a primitive form of wealth. *Proc. Natl. Acad. Sci. U. S. A.* 110, 15788–15793
- Newey, W.K. and Powell, J.L. (1987) Asymmetric least squares estimation and testing. *Econometrica* 55, 819–847
- Koenker, R. and Hallock, K.F. (2001) Quantile regression. *J. Econ. Perspect.* 15, 143–156
- Boyd, S. and Vandenberghe, L. (2004) *Convex Optimization*, Cambridge University Press
- Bottou, L. (1998) Online learning and stochastic approximations. In *On-line Learning in Neural Networks* (Vol. 9) (Saad, D., ed.), pp. 9–42, Cambridge University Press
- Sutton, R.S. and Barto, A.G. (1981) Toward a modern theory of adaptive networks: expectation and prediction. *Psychol. Rev.* 88, 135–170
- Aigner, D.J. et al. (1976) On the estimation of production frontiers: maximum likelihood estimation of the parameters of a discontinuous density function. *Int. Econ. Rev.* 17, 377–396
- Schultz, W. et al. (1997) A neural substrate of prediction and reward. *Science* 275, 1593–1599
- Niv, Y. (2009) Reinforcement learning in the brain. *J. Math. Psychol.* 53, 139–154
- Watabe-Uchida, M. et al. (2017) Neural circuitry of reward prediction error. *Annu. Rev. Neurosci.* 40, 373–394

Outstanding Questions

Under what circumstances do animals use reward distributions, rather than expected values (utility) in making decisions? How does distributional RL support changes in risk preferences?

Are optimistic and pessimistic value predictors explicitly specified during neural development? Are they organized in a topographic fashion in the mesostriatal dopamine pathway?

Do distributional TD errors in the brain improve animals’ representations of states in the environment, as they do in artificial systems?

How do quantile-like codes compare quantitatively with existing probabilistic population coding theories, such as PPCs and DDCs?

Are learning rates modulated by environmental volatility in a way that preserves the optimism or pessimism of individual value channels?

Might other neuromodulatory systems beyond dopamine, such as acetylcholine, be sensitive to the distribution of predicted events? If so, what kinds of codes are used to signal them?

What are the rules governing plasticity in neurons that receive dopamine input, particularly D1 and D2 receptor-expressing medium spiny neurons, in response to positive and negative dopamine transients? Do these rules serve to enhance distributional RL?

Biased value predictions and belief updating are associated with clinical anxiety, depression, addiction, and bipolar disorder. Do these biases arise from distributional RL and, if so, could interventions specifically targeting optimistic or pessimistic neurons help ameliorate them?

24. Dayan, P. and Daw, N.D. (2008) Decision theory, reinforcement learning, and the brain. *Cogn. Affect. Behav. Neurosci.* 8, 429–453
25. Lee, D. *et al.* (2012) Neural basis of reinforcement learning and decision making. *Annu. Rev. Neurosci.* 35, 287–308
26. Kable, J.W. and Glimcher, P.W. (2009) The neurobiology of decision: consensus and controversy. *Neuron* 63, 733–745
27. Watabe-Uchida, M. and Uchida, N. (2018) Multiple dopamine systems: weal and woe of dopamine. *Cold Spring Harb. Symp. Quant. Biol.* 83, 83–95
28. Cox, J. and Witten, I.B. (2019) Striatal circuits for reward learning and decision-making. *Nat. Rev. Neurosci.* 20, 482–494
29. Verharen, J.P.H. *et al.* (2020) Aversion hot spots in the dopamine system. *Curr. Opin. Neurobiol.* 64, 46–52
30. Klaus, A. *et al.* (2019) What, if, and when to move: basal ganglia circuits and self-paced action initiation. *Annu. Rev. Neurosci.* 42, 459–483
31. Berke, J.D. (2018) What does dopamine mean? *Nat. Neurosci.* 21, 787–793
32. Coddington, L.T. and Dudman, J.T. (2019) Learning from action: reconsidering movement signaling in midbrain dopamine neuron activity. *Neuron* 104, 63–77
33. Tian, J. *et al.* (2016) Distributed and mixed information in mono-synaptic inputs to dopamine neurons. *Neuron* 91, 1374–1389
34. Eshel, N. *et al.* (2016) Dopamine neurons share common response function for reward prediction error. *Nat. Neurosci.* 19, 479–486
35. Engelhard, B. *et al.* (2019) Specialized coding of sensory, motor and cognitive variables in VTA dopamine neurons. *Nature* 570, 509–513
36. Kim, H.R. *et al.* (2019) A unified framework for dopamine signals across timescales. *bioRxiv* Published online October 15, 2019. <https://doi.org/10.1101/803437>
37. Eshel, N. *et al.* (2015) Arithmetic and local circuitry underlying dopamine prediction errors. *Nature* 525, 243–246
38. Tian, J. and Uchida, N. (2015) Habenula lesions reveal that multiple mechanisms underlie dopamine prediction errors. *Neuron* 87, 1304–1316
39. Li, H. *et al.* (2019) Three rostromedial tegmental afferents drive triply dissociable aspects of punishment learning and aversive valence encoding. *Neuron* 104, 987–999
40. Prensa, L. and Parent, A. (2001) The nigrostriatal pathway in the rat: a single-axon study of the relationship between dorsal and ventral tier nigral neurons and the striosome/matrix striatal compartments. *J. Neurosci.* 21, 7247–7260
41. Matsuda, W. *et al.* (2009) Single nigrostriatal dopaminergic neurons form widely spread and highly dense axonal arborizations in the neostriatum. *J. Neurosci.* 29, 444–453
42. Rodríguez-López, C. *et al.* (2017) The mesoaccumbens pathway: a retrograde labeling and single-cell axon tracing analysis in the mouse. *Front. Neuroanat.* 11, 25
43. Smith, R.J. *et al.* (2019) Gene expression and neurochemical characterization of the rostromedial tegmental nucleus (RMTg) in rats and mice. *Brain Struct. Funct.* 224, 219–238
44. Zhou, T.C. *et al.* (2009) The rostromedial tegmental nucleus (RMTg), a GABAergic afferent to midbrain dopamine neurons, encodes aversive stimuli and inhibits motor responses. *Neuron* 61, 786–800
45. Otomo, K. *et al.* (2020) Subthreshold repertoire and threshold dynamics of midbrain dopamine neuron firing in vivo. *bioRxiv* Published online May 3, 2020. <https://doi.org/10.1101/2020.04.06.028829>
46. Yagishita, S. *et al.* (2014) A critical time window for dopamine actions on the structural plasticity of dendritic spines. *Science* 345, 1616–1620
47. Iino, Y. *et al.* (2020) Dopamine D2 receptors in discrimination learning and spine enlargement. *Nature* 579, 555–560
48. Behrens, T.E.J. *et al.* (2007) Learning the value of information in an uncertain world. *Nat. Neurosci.* 10, 1214–1221
49. Matias, S. *et al.* (2017) Activity patterns of serotonin neurons underlying cognitive flexibility. *Elife* 6, e20552
50. Doya, K. (2002) Metalearning and neuromodulation. *Neural Netw.* 15, 495–506
51. Monosov, I.E. (2017) Anterior cingulate is a source of valence-specific information about value and uncertainty. *Nat. Commun.* 8, 134
52. O'Neill, M. and Schultz, W. (2010) Coding of reward risk by orbitofrontal neurons is mostly distinct from coding of reward value. *Neuron* 68, 789–800
53. Hunnicutt, B.J. *et al.* (2016) A comprehensive excitatory input map of the striatum reveals novel functional organization. *Elife* 5, e19103
54. Soltani, A. and Izquierdo, A. (2019) Adaptive learning under expected and unexpected uncertainty. *Nat. Rev. Neurosci.* 20, 635–644
55. Bechara, A. *et al.* (1994) Insensitivity to future consequences following damage to human prefrontal cortex. *Cognition* 50, 7–15
56. Poletti, M. *et al.* (2010) Decision making in de novo Parkinson's disease. *Mov. Disord.* 25, 1432–1436
57. Kish, S.J. *et al.* (1988) Uneven pattern of dopamine loss in the striatum of patients with idiopathic Parkinson's disease. Pathophysiology and clinical implications. *N. Engl. J. Med.* 318, 876–880
58. Poletti, M. *et al.* (2011) Iowa gambling task in Parkinson's disease. *J. Clin. Exp. Neuropsychol.* 33, 395–409
59. Castrioto, A. *et al.* (2015) Iowa gambling task impairment in Parkinson's disease can be normalised by reduction of dopaminergic medication after subthalamic stimulation. *J. Neurol. Neurosurg. Psychiatry* 86, 186–190
60. Fiorillo, C.D. *et al.* (2003) Discrete coding of reward probability and uncertainty by dopamine neurons. *Science* 299, 1898–1902
61. Preusschoff, K. *et al.* (2006) Neural differentiation of expected reward and risk in human subcortical structures. *Neuron* 51, 381–390
62. Zalocusky, K.A. *et al.* (2016) Nucleus accumbens D2R cells signal prior outcomes and control risky decision-making. *Nature* 531, 642–646
63. Fiorillo, C.D. (2013) Two dimensions of value: dopamine neurons represent reward but not aversiveness. *Science* 341, 546–549
64. Schultz, W. *et al.* (2008) Explicit neural signals reflecting reward uncertainty. *Philos. Trans. R. Soc. Lond. B Biol. Sci.* 363, 3801–3811
65. St Onge, J.R. and Floresco, S.B. (2009) Dopaminergic modulation of risk-based decision making. *Neuropsychopharmacology* 34, 681–697
66. Nasrallah, N.A. *et al.* (2011) Risk preference following adolescent alcohol use is associated with corrupted encoding of costs but not rewards by mesolimbic dopamine. *Proc. Natl. Acad. Sci. U. S. A.* 108, 5466–5471
67. Mavrin, B. *et al.* (2019) Distributional reinforcement learning for efficient exploration. In *Proceedings in International Conference on Machine Learning*, pp. 4424–4434
68. Lyle, C. *et al.* (2019) A comparative analysis of expected and distributional reinforcement learning. In *Proceedings of the AAAI Conference on Artificial Intelligence* (33), pp. 4504–4511
69. Matsumoto, H. *et al.* (2016) Midbrain dopamine neurons signal aversion in a reward-context-dependent manner. *Elife* 5, e17328
70. Li, Y. and Dudman, J.T. (2013) Mice infer probabilistic models for timing. *Proc. Natl. Acad. Sci. U. S. A.* 110, 17154–17159
71. Starkweather, C.K. *et al.* (2017) Dopamine reward prediction errors reflect hidden-state inference across time. *Nat. Neurosci.* 20, 581–589
72. Starkweather, C.K. *et al.* (2018) The medial prefrontal cortex shapes dopamine reward prediction errors under state uncertainty. *Neuron* 98, 616–629
73. Ma, W.J. *et al.* (2006) Bayesian inference with probabilistic population codes. *Nat. Neurosci.* 9, 1432–1438
74. Pouget, A. *et al.* (2013) Probabilistic brains: knowns and unknowns. *Nat. Neurosci.* 16, 1170–1178
75. Sahani, M. and Dayan, P. (2003) Doubly distributional population codes: simultaneous representation of uncertainty and multiplicity. *Neural Comput.* 15, 2255–2279
76. Vértés, E. and Sahani, M. (2018) Flexible and accurate inference and learning for deep generative models. In *Advances in Neural Information Processing Systems* (31), pp. 4166–4175, MIT Press
77. Beck, J.M. *et al.* (2011) Marginalization in neural circuits with divisive normalization. *J. Neurosci.* 31, 15310–15319
78. Tversky, A. and Kahneman, D. (1992) Advances in prospect theory: cumulative representation of uncertainty. *J. Risk Uncertain.* 5, 297–323

79. Constantinople, C.M. *et al.* (2019) An analysis of decision under risk in rats. *Curr. Biol.* 29, 2066–2074
80. Mikhael, J.G. and Bogacz, R. (2016) Learning reward uncertainty in the basal ganglia. *PLoS Comput. Biol.* 12, e1005062
81. Gershman, S.J. and Uchida, N. (2019) Believing in dopamine. *Nat. Rev. Neurosci.* 20, 703–714
82. Babayan, B.M. *et al.* (2018) Belief state representation in the dopamine system. *Nat. Commun.* 9, 1891
83. Lak, A. *et al.* (2017) Midbrain dopamine neurons signal belief in choice accuracy during a perceptual decision. *Curr. Biol.* 27, 821–832
84. Sarno, S. *et al.* (2017) Dopamine reward prediction error signal codes the temporal evaluation of a perceptual decision report. *Proc. Natl. Acad. Sci. U. S. A.* 114, E10494–E10503
85. Fiorillo, C.D. *et al.* (2013) Diversity and homogeneity in responses of midbrain dopamine neurons. *J. Neurosci.* 33, 4693–4709
86. Yamins, D.L.K. *et al.* (2014) Performance-optimized hierarchical models predict neural responses in higher visual cortex. *Proc. Natl. Acad. Sci. U. S. A.* 111, 8619–8624
87. Bashivan, P. *et al.* (2019) Neural population control via deep image synthesis. *Science* 364, eaav9436
88. Bertsekas, D.P. and Tsitsiklis, J.N. (1996) *Neuro-Dynamic Programming* (1st edn), Athena Scientific
89. Rowland, M. *et al.* (2019) Statistics and samples in distributional reinforcement learning. In *Proceedings in International Conference on Machine Learning*, pp. 5528–5536